Ecotoxicology and Environmental Safety 184 (2019) 109604

Contents lists available at ScienceDirect

Ecotoxicology and Environmental Safety

journal homepage: www.elsevier.com/locate/ecoenv

Profiles, source identification and health risks of potentially toxic metals in pyrotechnic-related road dust during Chinese New Year

Shaochen Yang[a], Ping Li[b], Jinling Liu[a,*], Xiangyang Bi[a], Yongqiang Ning[a], Sheng Wang[a], Pengcong Wang[a]

[a] Hubei Key Laboratory of Critical Zone Evolution, School of Earth Sciences, China University of Geosciences, Wuhan, 430074, China
[b] State Key Laboratory of Environmental Geochemistry, Institute of Geochemistry, Chinese Academy of Sciences, Guiyang, 550081, China

ARTICLE INFO

Keywords:
Potentially toxic metal
Pyrotechnic display
Road dust
Human health risk

ABSTRACT

Potentially toxic metal (PTM) pollution in road dust is of great concern, however, our understanding of PTMs released by pyrotechnic displays and their adverse impacts on human health in road dust is limited. Here, we studied PTM pollution levels and Pb isotope signatures in pyrotechnic ash and road dust (aged dust and pyrotechnic-influenced dust) samples from eight cities in China during Chinese New Year and carried out a human health risk assessment. Pyrotechnic ash had higher values of Cr, Co, Ni, Cu, Zn, As, Sr and Pb but lower values of Mn and Cd than Chinese background soil. Pyrotechnic-influenced dust had significantly higher Cu and Cr values than aged dust, with enrichment of Sr, Cu, Pb, Cr and Ni in road dust after pyrotechnic displays. Both $^{208}Pb/^{206}Pb$ and Sr values were used to confirm the presence of pyrotechnic ash in road dust. A positive matrix factorization demonstrated that pyrotechnic events contributed 70.1%, 50.4%, 36.6% and 35.5% of the Sr, Cu, Cr and Pb values to these road dust, respectively. We found that non-carcinogenic and carcinogenic risks related to PTMs in road dust were at safe levels during the Chinese New Year, although both risks were elevated following pyrotechnic events. Typically, PTM pollutants related to pyrotechnic events contributed 33.99% to non-carcinogenic and 21.83% to carcinogenic risks, suggesting that more attention needs to be paid to this source of PTM pollution in China. Current results improve our understanding of PTM pollution in pyrotechnic-influenced road dust and health risks related to pyrotechnic displays in China.

1. Introduction

Environmental chemical pollutants such as elemental carbon, organic carbon and potentially toxic metals (PTMs) in $PM_{2.5}$, PM_{10} or road dust are potentially toxic to populations (Luo et al., 2011; Pongpiachan et al., 2015) and can significantly affect the hospital admission numbers (Pongpiachan and Paowa, 2014). Among these chemical pollutants, PTMs can remain in urban environments for a long time, posing a potential toxic threat to the surrounding ecosystem and acting as a source of secondary pollution (Luo et al., 2011). Numerous previous works have studied PTM fractions, sources and health risks in $PM_{2.5}$ and PM_{10} in the atmosphere (Gao et al., 2018; Huang et al., 2018; Luo et al., 2019). However, road dust, which acts as an important source and sink of PTMs (Hu et al., 2015; Li et al., 2017a), has recently become a major health concern. The primary sources of PTMs in road dust have been reported to be vehicle exhaust emissions, industrial emissions, brake wear, coal combustion, metallurgical processes and waste from municipal construction (Gunawardana et al., 2012; Pongpiachan et al., 2015). However, pyrotechnic displays, which are used to celebrate events around the world, may contribute unusual PTMs to road dust because of the enrichment of PTMs in pyrotechnic materials (Vecchi et al., 2008). This is especially true in China, where numerous pyrotechnic activities are carried out during Chinese New Year (Cao et al., 2017). To enhance displays, pyrotechnic devices are generally spiked with specific metal elements, like strontium (Sr), lead (Pb) or copper (Cu) (Cao et al., 2017). Following pyrotechnic displays, some of these ashed PTMs aggregate into coarser particles are deposited as road dust (up to 6 h afterwards). These particles pose potential risks to human health via dust exposure over a long time (Crespo et al., 2012; Cao et al., 2017). Previous studies have focused on the air pollution generated by pyrotechnic displays (both long-term and short-term) and its hazardous impact on human health (Pongpiachan et al., 2017a, 2018). Clearly, to investigate the environmental effect and fate of PTMs emitted during pyrotechnic displays comprehensively, pyrotechnic-influenced road dust needs to be rigorously investigated.

Many studies in the past have investigated the emission strength,

* Corresponding author.
E-mail address: liujinling@cug.edu.cn (J. Liu).

https://doi.org/10.1016/j.ecoenv.2019.109604
Received 22 May 2019; Received in revised form 3 August 2019; Accepted 22 August 2019
Available online 29 August 2019

pollutants, particle size distribution, noise effects and health risks related to pyrotechnic displays (Jing et al., 2014; Pongpiachan and Iijima, 2016; Pongpiachan et al., 2018; Yang et al., 2014b). However, few have carried out qualitative source identification of PTMs and fewer still have carried out quantitative source apportionment of these PTMs in road dust. Currently, studies of pyrotechnic-related pollutants have used morphological characteristics (Azhagurajan et al., 2014), specific elements (such as Sr) (Vecchi et al., 2008), principal component analysis (PCA) (Pongpiachan et al., 2017a) and enrichment factors (EFs) to identify natural versus pyrotechnic sources (Luo et al., 2015; Pongpiachan et al., 2018). In addition, high values of Pb are also associated with pyrotechnic materials (Gurugubelli, 2014). Nevertheless, information on Pb isotope ratios that would be useful for tracing pyrotechnic sources is limited. Generally, both $^{208}Pb/^{206}Pb$ and $^{206}Pb/^{207}Pb$ ratios are used as environmental tracers because of their relative abundances and invariance to physio-chemical processes (Bi et al., 2017; Cheng and Hu, 2010; Das et al., 2018). Since anthropogenic Pb usually has distinctive $^{206}Pb/^{207}Pb$ and $^{208}Pb/^{206}Pb$ ratios compared with natural materials (Cheng and Hu, 2010; Widory et al., 2010), it is feasible to identify pyrotechnic-influenced dust using Pb isotopes (Bi et al., 2017; Cundy and Croudace, 2017; Martinez-Haro et al., 2011). However, methods for assessing pyrotechnic-related PTM pollution have limited quantitative capabilities. Accordingly, an effective receptor model, such as positive matrix factorization (PMF) based on principle component analysis, can provide information on the practical contribution rates of different sources, in contrast to other receptor models (e.g., chemical mass balances; multiple linear regression) (Comero et al., 2014; Huang et al., 2018). Compared with other statistical techniques, PMF can use realistic error estimates of data values and provide a more reliable way of assessing the quantitative contribution of each source (Huang et al., 2018). In environmental work, some degree of robustness is achieved using PMF through judicious use of error estimates. However, this is not straight forward for first-time users (Paatero and Tapper, 1994). We found that no single statistical method provided comprehensive information on PTM pollution; therefore, EFs, isotope methods, specific element concentrations and PMF were combined to accurately identify PTM pollution related to pyrotechnics.

Typical PTMs emitted during pyrotechnic displays are expected to effect human health because of their chemical properties (Baranyai et al., 2015). $PM_{2.5}$ derived PTMs from pyrotechnics were reported to have short-term health effects (Crespo et al., 2012), mainly related to exposure via inhalation of the smoke (Cao et al., 2017). However, pyrotechnic-related PTMs in road dust may be solubilized in urban runoff (especially under low pH) and affect the quality of receiving water, posing a long-term health effect (Liu et al., 2014), especially in the case of bioaccessible PTMs (Luo et al., 2012). Thus, it is necessary to account for a more realistic exposure of pyrotechnic-related PTMs to biota via road dust. Bioaccessibility of PTMs is commonly assessed via extraction methods (e.g., the simple bioaccessibility extraction test (SBET), *in vitro* gastrointestinal test, physiologically based extraction test and unified bioaccessibility methods) to determine the adverse health effects of exposure to road dust (Bi et al., 2015; Ettler et al., 2019; Oomen et al., 2002; Padoan et al., 2017). To date, few studies have made quantitative bioaccessible evaluations or assessed the pyrotechnic-related PTM contribution to human health risks (Cao et al., 2017). Therefore, a realistic assessment of the integrated actual health risks associated with pyrotechnic-related PTMs in road dust is yet to be carried out.

Given that Cr, Mn, Co, Ni, Cu, Zn, As, Sr, Pb and Cd are usually considered environmental hazards in pyrotechnics (Cao et al., 2017; Vecchi et al., 2008), this study focuses on these PTMs in typical pyrotechnic ash samples, as well as road dust samples, collected before and after pyrotechnic displays in eight cities of China during Chinese New Year. The study aims to: 1) investigate the characteristics of PTMs in pyrotechnic ash and road dust during pyrotechnic displays; 2) determine the contribution of pyrotechnic materials to PTM levels in road dust; and 3) assess the bioaccessible risks and evaluate exposure levels to PTMs in road dust containing material derived from pyrotechnic displays.

2. Materials and methods

2.1. Study area and sample preparation

Pyrotechnic displays are very popular in China, especially during Chinese New Year. In this study, eight cities distributed throughout China, including Xi'an (XA), Dezhou (DZ), Shijiazhuang (SJZ), Jinzhong (JZ), Ganzhou (GZ), Changsha (CS), Ledong (LD) and Xuanwei (XW) (Fig. S1), were selected as sampling sites to evaluate the effects of pyrotechnic events on PTM contamination in road dust. Sampling was conducted before and after Chinese New Year of 2017. Weather conditions during sampling at each site are recorded in Table S1.

A total of 66 dust samples and 67 pyrotechnic ash-residue samples were collected. At each sampling site, triplicate road dust samples were collected before and after pyrotechnic displays related to Chinese New Year. Road dust collected before these pyrotechnic events were defined as aged dust (n = 33), while those collected afterwards were designated pyrotechnic-influenced dust (n = 33). Dust samples were collected using brushes and a shovel and were placed in sealed bags and transferred to the laboratory. Samples were left to air-dry at room temperature, before removing stones and leaves from all samples and gently sieving all remaining material through a 100-mesh sieve (Lin et al., 2017). Pyrotechnic devices were purchased in Hunan, where most pyrotechnic production occurs within China. A total of 11 representative types of pyrotechnic devices (fireworks and firecrackers) were selected and burned to obtain ash samples (n = 67). Pyrotechnic ash were also stored in sealed bags, transported to the laboratory and prepared for analyses.

Both road dust (50 mg) and pyrotechnic ash (50 mg) samples were dissolved in a mixture of concentrated HF (40%, v/v) and HNO_3 (65%, v/v) in an oven at 190 °C over 48 h (Bi et al., 2015). These solutions were cooled, filtered and diluted by HNO_3 (2%, v/v) to analyze their concentrations of trace elements using an inductively coupled plasma mass spectrometer (ICP-MS; Agilent 7900; Agilent Technologies, Santa Clara, CA, USA). To ensure analytical quality, duplicate samples, reagent blanks and sediment reference materials (GBW-07423) were analyzed along with samples. The recoveries of reference materials were within the range of 85%–115% for the measured elements (Table S2). The relative standard deviations (RSDs) of replicate samples were lower than 10%. A total of 19 samples with higher Pb contents, including seven pyrotechnic ash, six pyrotechnic-influenced dust and six aged dust from both southern and northern sampling sites were selected to determine Pb isotope ratios using the ICP-MS, following the protocol described in our previous study (Bi et al., 2015). Details of the Pb isotope analysis are provided in the Supporting Information (SI; Methods used for sample analysis). To determine the bioaccessibility of PTMs in this study, the SBET was used. Details of the SBET also are presented in the SI (Methods used for sample analysis).

2.2. Enrichment factors

EFs were used to evaluate the impact of pyrotechnic displays and other anthropogenic activities on road dust (Li et al., 2019; Luo et al., 2015). In prior studies, Al, Si and Fe were widely used for the EF calculations (Pongpiachan et al., 2017b). In this study, Al was adopted as the reference element to assess EFs in road dust samples. EFs were calculated using Eq. (1) (Pongpiachan et al., 2017b):

$$EF = \frac{(C_i/C_r)_{sample}}{(C_i/C_r)_{background}} \quad (1)$$

where C_r is the value of the reference element and C_i is the value of element i. This study uses the background soil values of China as a reference.

2.3. Positive matrix factorization

PMF was applied to quantify and identify the main sources of PTMs in road dust samples following pyrotechnic displays at each site. Concentrations of the PTMs and their uncertainty were input into the PMF model (Huang et al., 2018). The identification of sources was based on tracers, while their contributions were estimated by finding optimal solutions to the PMF model. Generally, PMF is an efficient multivariate factor analysis method for the identification sources (Yu et al., 2016a). In the PMF model, the sample content matrices are decomposed into factor profile matrices versus factor contribution matrices. Based on the results of this decomposition, the profile information collected and emission inventories, sources can be evaluated (Yu et al., 2016b). PMF was calculated using the following Eq. (2):

$$\mathrm{xij} = \sum_{k=1}^{p} \mathrm{gikfkf} + \mathrm{eij} \tag{2}$$

where x_{ij} is the content of species j measured in sample I, p is the number of factors, g_{ik} is the relevant contribution of factor k to sample i, f_{kf} is the concentration of species j in factor profile k, and e_{ij} is the residual.

Factor profiles and concentrations are obtained from the PMF model by minimizing the objective function Q as defined in Eq. (3) (Tian et al., 2013).

$$Q = \sum_{i=1}^{n} \sum_{j=1}^{m} \left(\frac{eij}{uij}\right)^2 \tag{3}$$

where u_{ij} is the uncertainly (Chen et al., 2016a), which is calculated using Eq. (4):

$$uij = \begin{cases} \frac{5}{6} \times \mathrm{MDL}, & \mathrm{xij} \le \mathrm{MDL} \\ \sqrt{(\sigma j \times xij)^2 + (\mathrm{MDL})^2}, & \mathrm{xij} > \mathrm{MDL} \end{cases} \tag{4}$$

where x_{ij} is the concentration of species j in sample i, and σ_j is the relative standard deviation of the concentrations of species j.

2.4. Human health risk assessment

To assess the probability of non-carcinogenic and carcinogenic risks to humans related to PTMs in road dust derived from pyrotechnic events, we selected the human health risk assessment model established by the US Environmental Protection Agency (EPA) for assessing levels of contaminants in soils under various urban exposure conditions (USEPA, 1989, Table S3). According to this model, the non-carcinogenic daily intake is divided into three pathways, involving ingestion, inhalation and dermal contact. In this model, metal exposure via ingestion is usually estimated using bioaccessible metal values from recent studies (Li et al., 2017a; Wang et al., 2016). To evaluate carcinogenic risks, the lifetime averaged daily dose (LADD) for Ni, Cr and Cd inhalation exposure routes was applied (Keshavarzi et al., 2015). Details of health risk assessments for various trace elements and emission sources are described in the SI (Details of health risk assessment).

2.5. Data analysis

All statistical analyses were performed using Excel 2016 and SPSS 19.0 for Windows. Analysis of variance (ANOVA) was conducted to investigate whether there were any significant differences in PTM contents among samples. Bi-variate relationships between different variables were determined and p values of < 0.05 were considered statistically significant. Sources of PTMs in road dust were analyzed using the EPA PMF model version 5.0. Up to 20 runs were used to

Table 1
Concentrations of potentially toxic metals in different types of pyrotechnic ashes (mg/kg, mean ± 1σ).

Pyrotechnic ashes type	Cr	Mn	Co	Ni	Cu	Zn	Sr	Mo	Pb	As
XNB (n = 1)	652	315	88.7	4.23	184	687	1005	0.371	522	26.8
ABB (n = 3)	1187 ± 103	362.6 ± 35.7	11.7 ± 0.157	16.1 ± 1.38	6538 ± 93	149 ± 4.16	12030 ± 375	35.8 ± 5.92	661.8 ± 10.7	55.1 ± 28.5
XYX (n = 3)	246 ± 19.7	320 ± 19.8	1.19 ± 0.191	2.93 ± 0.103	11638 ± 1218	60.0 ± 2.24	2698 ± 559	9.4 ± 0.115	< 0.01	17.5 ± 12.3
DTEZ (n = 4)	2102 ± 63.5	601 ± 30.2	218 ± 5.12	8.46 ± 0.244	9558 ± 267	144 ± 18.2	3557 ± 377	27.6 ± 6.41	643 ± 14.8	37.2 ± 21.9
HDY (n = 3)	13520 ± 2679	644 ± 67.9	29.5 ± 23.4	101 ± 24.3	173760 ± 12732	589 ± 31.8	13925 ± 935	44.2 ± 3.96	1884 ± 416	42.5 ± 16.2
QHYC (n = 9)	855 ± 423	478 ± 128	12.9 ± 6.13	21.4 ± 11.0	7705 ± 3195	< 0.01	1777 ± 749	74.5 ± 41.1	2.45 ± 1.96	60.7 ± 15.7
JHQJ (n = 10)	4129 ± 1200	361 ± 125	95.3 ± 76.1	115 ± 81.3	58690 ± 25734	324 ± 220	11386 ± 5151	362 ± 161	6.67 ± 3.15	18.4 ± 5.4
KQKP (n = 8)	1918 ± 197	855 ± 57.1	3.35 ± 0.712	37.1 ± 27.8	14891 ± 2111	271 ± 195	2454 ± 813	32.6 ± 5.55	79.9 ± 76.2	21.2 ± 3.1
QYJZ (n = 8)	574 ± 164	568 ± 96.3	2.44 ± 1.23	0.454 ± 0.214	3631 ± 1018	315 ± 128	4798 ± 1660	2.24 ± 1.97	52.5 ± 30.2	31.9 ± 6.0
HKFD (n = 2)	1759 ± 606	604 ± 236	111 ± 110	12.4 ± 1.5	33667 ± 2460	161 ± 12.5	15242 ± 2577	98.2 ± 74.3	3.35 ± 0.977	82.7 ± 13.4
DDH (n = 9)	910 ± 159	727 ± 179	6.12 ± 1.33	8.31 ± 1.17	394 ± 26.0	489 ± 40.5	38.1 ± 1.43	2.81 ± 0.0117	74.4 ± 30.5	14.5 ± 1.2
All samples	2532 ± 3798	530 ± 178	52.7 ± 68.8	29.7 ± 40.1	29150 ± 50977	289 ± 219	6264 ± 5674	62.7 ± 103	357 ± 573	37.1 ± 21.5

analyze samples of this study, in which the species were categorized as "Strong", "Weak" and "Bad" based on their signal to noise ratio. If the values of scaled residuals for all the elements were within the range from −3 to +3 and the difference between Q_{robust} and Q_{ture} was small, then the base run was regarded as stable. Unless otherwise stated, PTM values are expressed in mg/kg for all samples in this study.

3. Results and discussion

3.1. Potentially toxic metal concentrations in pyrotechnic ash

Descriptive statistics of PTM values in all 11 types of pyrotechnic ash are presented in Table 1. Values of PTMs in pyrotechnic ash decreased in the order of Cu > Sr > Cr > Mn > Pb > Zn > Mo > Co > As > Ni > Cd. Values of Cu and Cr in pyrotechnic ash were 50 and 1441 times higher than those in the Chinese background soil (CNEMC , 1990). A significant correlation ($r^2 = 0.41$, $p < 0.01$) was observed between $\log_{10}C_{Cu}$ and $\log_{10}C_{Cr}$ in pyrotechnic ash samples (Fig. S2), which is attributed to the presence of $CuCr_2O_4$ in pyrotechnic materials. During pyrotechnic displays, Cu gives a blue flame, while $CuCr_2O_4$ acts as a catalyst for the propellants (Vecchi et al., 2008; Zhang et al., 2016). In addition, Pb was abundant in some fireworks, e.g., HDY, ABB and DTEZ types, with the highest value of 3384 ± 216 mg/kg recorded for the HDY firework ash. This value was also 130 times higher than that of the Chinese background soil (CNEMC , 1990), suggesting Cr, Cu and Pb in pyrotechnic devices are most likely to produce environmental toxicity. Similarly, Sr contents in pyrotechnic ash ranged from 1777 mg/kg to 15242 mg/kg, yielding values that were 57 times higher than that of the Chinese background soil (CNEMC , 1990). Mo, Ni, Co, Zn and As had potential environmental toxicity, with values that were 30, 1.1, 4.2, 3.9 and 3.4 times higher than those of the Chinese background soil (CNEMC , 1990). In addition, Ni in JHQJ, Co in DTEZ and Mo in HKFD had high levels compared with other pyrotechnic devices (Table 1), indicating distinct values of Ni, Co and Mo in different types of pyrotechnic devices. Moreover, Mn had lower values (530 ± 178 mg/kg) in pyrotechnic ash compared with the Chinese background soil (583 mg/kg, CNEMC , 1990), causing less environmental concern. Cd values in pyrotechnic ash were extremely low (< 0.1 ng/g), indicating Cd pollution was unrelated to pyrotechnic displays.

3.2. Potentially toxic metal concentrations and characteristics in pyrotechnic versus aged dust

The mean values of PTMs in road dust samples from eight cities during the pyrotechnic events of Chinese New Year in 2017 are shown in Table S4. Fig. 1 presents the values of the most concerning toxic metals in road dust (Cr, Ni, Cu, Zn and Pb) (Hu et al., 2015). To assess the temporal distribution of these five PTMs, a probability distribution function (PDF) was applied to samples collected from all eight cities during Chinese New Year. The PDF function describes the relative probability of a random variable having the measured concentrations (Pongpiachan and Iijima, 2016):

$$y = \frac{1}{\sigma\sqrt{2\pi}}\exp\left(\frac{-(x-\mu)^2}{2\sigma^2}\right) \quad (5)$$

where y, σ, σ^2 and x represent the PDF value, standard deviation, variance, mean and road dust concentration of each selected PTM, respectively. As a part of the analysis, skewness was used to evaluate the asymmetry of the probability distribution of each selected PTM in the road dust samples. In the case of a unimodal distribution, a positive skew suggests that the tail on the right side of the PDF is longer than the left side, indicating the mean of the selected metal is lower than the middle value. Meanwhile, a negative skew suggests that the tail on the left side is longer than the right side, indicating the mean of the selected PTM is greater than the middle value. Unusually high levels of a given PTM emitted from other sources would be responsible for these phenomena. If the mean lies in the middle, it is more likely to have a Gaussian distribution, indicating a conventional normal distribution without any PTM sources from other extreme events (Pongpiachan and Iijima, 2016).

The PDFs of the five selected PTMs in aged dust and pyrotechnic dust samples show several interesting features in Fig. 2. In aged dust, a symmetrical bell-shaped curve was detected for Cr, suggesting that the observed values are likely concentrated in the middle, rather than the tails. This reflects a strong homogeneous distribution of Cr in aged dust, which is less likely related to a specific pollution event. However, in pyrotechnic dust, Cr has a sharp positively skewed curve (the tail on the right side is much longer than the left), affirming the importance of pyrotechnic displays on Cr values in road dust. We found a similar trend in Cu values. However, Ni, Pb and Zn showed similar distributions in both aged and pyrotechnic dust. This is consistent with Fig. 1, which indicated that levels of Cu and Cr were more likely affected by pyrotechnic displays. Although Ni and Pb were specific to some pyrotechnic devices (Table 1), they clearly do not pose a widespread or significant environmental threat.

Similarly, the ANOVA analysis indicated that the Cu and Cr values in pyrotechnic-influenced dust were significantly higher than those in aged road dust (Cu: $p = 0.005$, Cr: $p = 0.003$), also suggesting Cu and Cr were the dominant PTM pollutants released to road dust through pyrotechnic events. Although Pb is commonly used to confirm reproducible and steady burning rates during pyrotechnic events, there was no significant difference between Pb values in the pyrotechnic-influenced dust and aged dust ($p = 0.617$). This could be partially explained by the fact that Pb_3O_4 has been replaced by a non-Pb-bearing catalyst (e.g., $Bi(NO_3)_3$ or Bi_2O_3) in some types of pyrotechnic devices (e.g., XYX, QHYC, HKFD and JHQJ), in accord with Chinese policy. There was no significant difference between some of the other PTMs (Zn and Ni) in pyrotechnic-influenced dust and aged dust (Zn: $p = 0.815$, Ni: $p = 0.133$), which is consistent with their relatively low toxicity in pyrotechnic ash and our PDF results. However, PTM contents in pyrotechnic-influenced dust in all eight cities were much lower than those of pyrotechnic ash samples. This reflects dilution of PTMs deposited as road dust and the loss of some fine particle PTMs during pyrotechnic displays (Crespo et al., 2012; Yang et al., 2014b).

In LD, Cr, Cu and Pb in pyrotechnic-influenced dust were 1.46, 3.75 and 1.68 times higher than those in aged road dust, suggesting more intense pyrotechnic-related pollution occurs in LD (Hainan). Moreover, Cr values in pyrotechnic-influenced dust of GZ were 9.45 times higher than those in aged dust (Table S4), suggesting very serious Cr pollution caused by pyrotechnic displays. These results indicate that more pyrotechnic activities may be carried out in southern China. To estimate the inter-site differences of selected PTMs among these eight cites, we computed coefficients of divergence (COD_{jk}), using Eq (6) (Pongpiachan and Iijima, 2016):

$$CODjk = \sqrt{\frac{1}{n}\sum_{i=1}^{n}\left(\frac{xij - xik}{xij + xik}\right)^2} \quad (6)$$

where x_{ij} indicates the values of selected metals in road dust during sampling event *i* at sampling sites *j*, x_{ik} is the value of selected metals in road dust during sampling event *i* at sampling sites *k*, and *n* is the total number of sampling events. COD values were determined for both long- and short-time measurements (Pongpiachan and Iijima, 2016). When COD values are close to 0, this suggests there is a strong similarity of emission sources between the two sampling sites; while COD values of close to 1 indicate dissimilarity between the two sites.

The majority of selected PTMs had relatively low COD values (< 0.36, Table S5), indicating that the road dust PTM levels at all eight sites were likely affected by comparable sources. However, Cu had a higher value of 0.41 among southern (LD, XW, GZ, CS) and northern cities (SJZ, JZ, DZ, XA), reflecting distinct sources of Cu in southern and

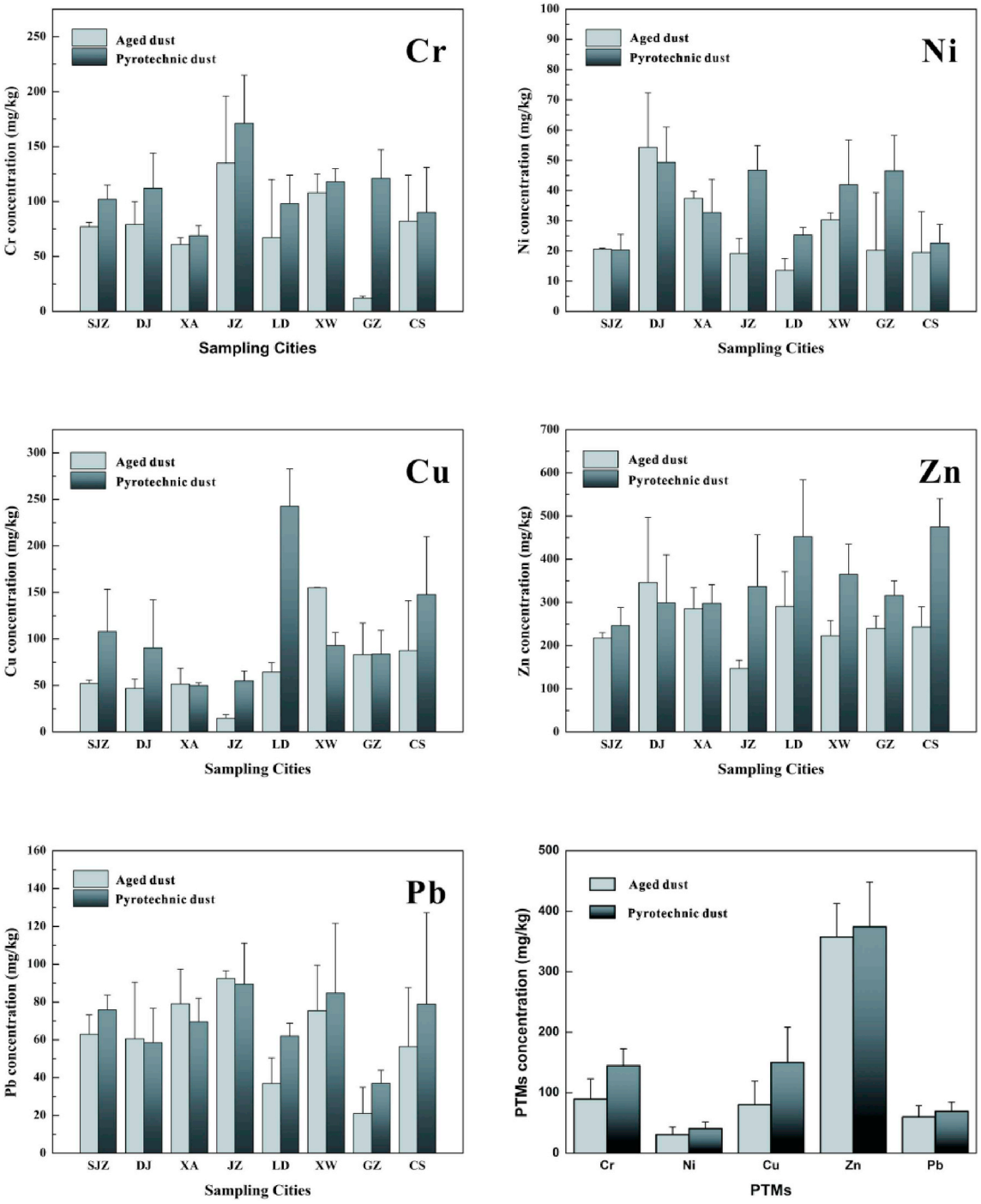

Fig. 1. Concentrations of Cr, Ni, Cu, Zn and Pb (mean ± 1σ) in aged dust and pyrotechnic dust samples from eight cities in China (aged dust: road dust sampled before pyrotechnic events; pyrotechnic dust: road dust sampled after pyrotechnic events).

northern Chinese cities. Because Cu was the most enriched PTM in pyrotechnic devices, different pyrotechnic displays would produce different Cu emission patterns. Thus, we concluded that the higher COD values for Cu reflect the fact that more pyrotechnic displays occurred in southern cities of China during Chinese New Year celebrations.

3.3. Source apportionment of potentially toxic metals in road dust

3.3.1. Enrichment factor analysis

The sequence of EFs for the 11 selected PTMs observed in road dust before pyrotechnic events was: Cd > Zn > Cu > As > Pb > Sr > Mn > Cr > Mo > Co > Ni, while after pyrotechnic events it was: Cd > Cu > Zn > Sr > As > Pb > Cr > Ni > Mn > Mo > Co (Table S6). According to previous work (Li et al., 2019), the EFs can be used to classify these elements into three categories, having: 1) EF < 3, that is, those that were not enriched (e.g., Co, Mo, Mn, Ni, Cr and Sr, Pb before pyrotechnic displays). 2) 3 < EF < 5, that is, those that had moderate enrichment (e.g., Zn, As, Cu before pyrotechnic displays; and Sr, Pb after pyrotechnic displays); and 3) 5 < EF < 25, i.e., those that showed marked enrichment (e.g., Cd and Cu after pyrotechnic displays). In this study, the EFs of Cu and Sr changed a lot following pyrotechnic events. Before the pyrotechnic displays, the EF of

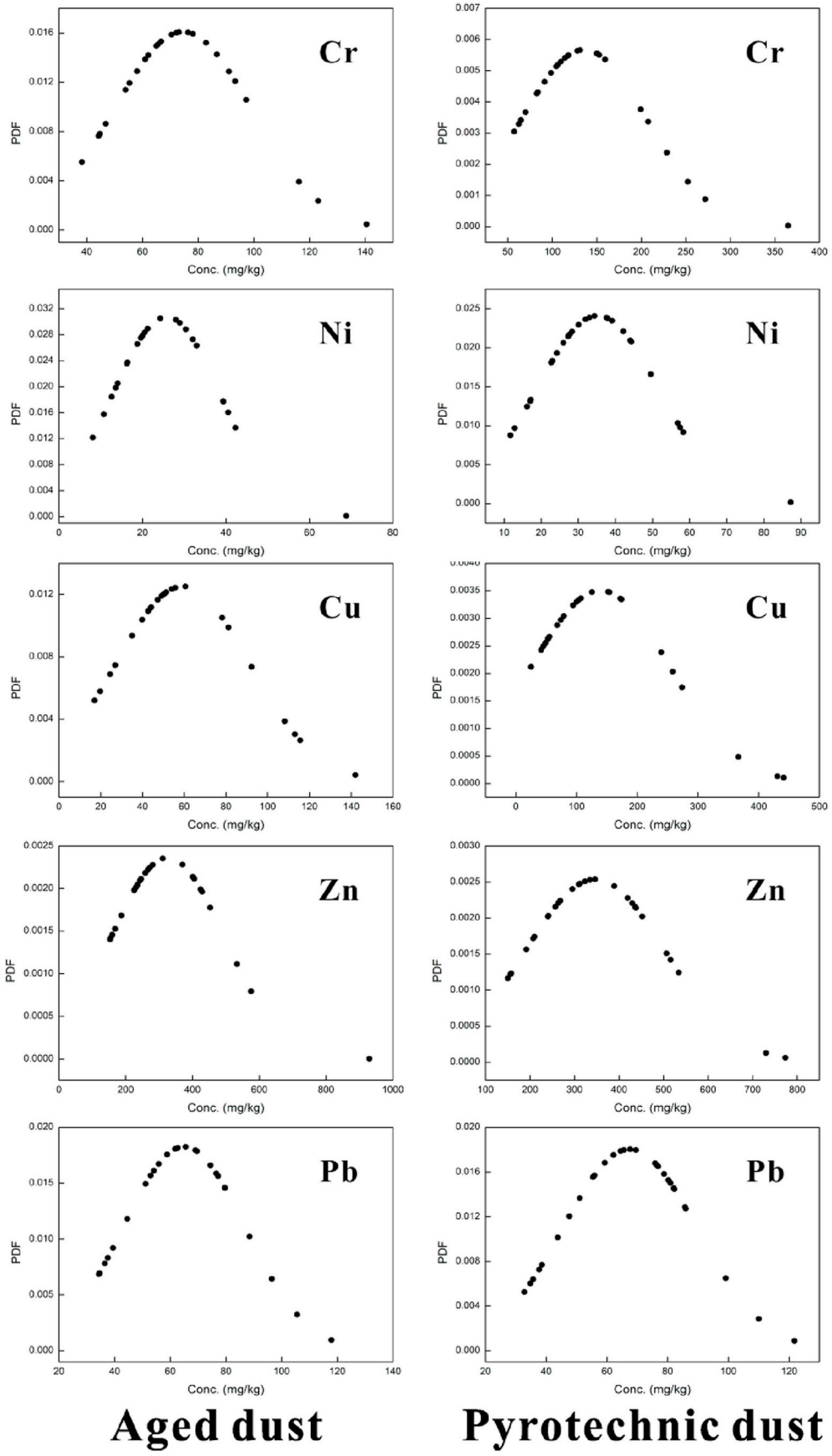

Fig. 2. Probability distribution functions of five selected metals collected from eight cities during Chinese New Year.

Cu was only 3.88, indicating a moderate pollution level; however, after the pyrotechnic displays, the EF of Cu rose to 9.54, suggesting pyrotechnic-related-Cu was present in the road dust; Similarly, the EF of Sr changed from 1.87 (low pollution) to 4.45 (moderate pollution) after the pyrotechnic events. Prior studies have reported similarly high values of Sr in $PM_{2.5}$ during the Chinese New Year and Lantern festivals, related to pyrotechnic events in Chengdu and Taiwan (Tang et al., 2013; Tsai et al., 2012). Therefore, we surmise that elevated Sr in the road dust of this study is likely related to pyrotechnic events. This result is consistent with elevated levels of Cu and Sr in pyrotechnic ash. Likewise, EFs of Pb, Cr and Ni in road dust after pyrotechnic displays were 1.27, 1.36 and 1.57 times higher than prior to these displays, indicating that these pyrotechnic-derived PTMs are non-negligible in road dust. Clearly, both Cd and Zn had high EFs in road dust prior to the pyrotechnic events. This was also observed in a previous study (Luo et al., 2015). Results presented in Section 3.1 suggest that Cd and Zn were not contributed to road dust by pyrotechnic ash, but likely have another anthropogenic source (e.g., traffic, coal combustion or industrial activities). Details of the source identification for all measured PTMs are discussed in Section 3.4.

3.3.2. Pb isotope analysis

In addition to pyrotechnic events, Pb could be derived from many other sources, including coal combustion, traffic, metal ores and other geological sources, resulting in it being difficult to identify a firework-origin based on Pb concentrations alone (Cao et al., 2017). However, a recent study suggested that stable Pb isotopic compositions could be used to characterize firework particles (Li et al., 2017b). Significant changes in Pb values were found in road dust samples from CS, LD and SJZ after pyrotechnic displays ($p = 0.011$), indicating potential Pb pollution related to pyrotechnic sources at sites CS, LD and SJZ. The Pb isotope compositions of pyrotechnic-influenced dust, aged road dust and pyrotechnic ash of this study, as well as other sources are presented in Fig. 3 and Table S7. We included Pb isotope ratios for vehicle exhausts (leaded and non-leaded types), coal combustion emissions, as well as background soils and ores of China from the literature (Bi et al., 2017).

The $^{206}Pb/^{207}Pb$ and $^{208}Pb/^{206}Pb$ ratios in pyrotechnic ash samples ranged from 1.164 to 1.177 and from 2.058 to 2.088, respectively. The $^{208}Pb/^{206}Pb$ values of pyrotechnic ash samples are obviously lower than those of vehicle exhausts (2.110–2.204), coal combustion emissions (2.100–2.220), background soils (2.072–2.085) and Chinese ores (2.089–2.190) (Fig. 3) (Bi et al., 2017). Aged road dust samples had $^{206}Pb/^{207}Pb$ ratios of 1.173–1.197 and $^{208}Pb/^{206}Pb$ ratios of 2.100–2.161, which lie within the range for Chinese coal combustion (Bi et al., 2017), indicating coal combustion is likely the main Pb source in aged road dust. After pyrotechnic events, the $^{208}Pb/^{206}Pb$ ratios of the road dust samples decreased to 2.092–2.131, clearly indicating the influence of pyrotechnic Pb emissions.

The ratios of $^{206}Pb/^{207}Pb$ of pyrotechnic-influenced dust, aged dust and pyrotechnic ash span a small range of 1.15–1.2. In this case, $^{206}Pb/^{207}Pb$ ratios may not work effectively as a tracer in this study, despite successfully tracing many other sources in various urban environments (Bi et al., 2017; Cheng and Hu, 2010). Therefore, we used both $^{208}Pb/^{206}Pb$ and Sr concentrations to discriminate pyrotechnic ash sources from other road dust sources. The $\log_{10}C_{Sr}$ values and $^{208}Pb/^{206}Pb$ ratios are plotted in Fig. 3. Using these values, we could differentiate all three sample types very well. In fact, Pb ratios of pyrotechnic-influenced dust lie between aged road dust and pyrotechnic ash values, demonstrating that pyrotechnic-influenced dust is a mixture of aged dust and deposited pyrotechnic ash.

The linear relationship among Pb isotope ratios and Sr contents of aged road dust, pyrotechnic-influenced dust and pyrotechnic ash samples suggests that pyrotechnic events are a principal local source of Pb in road dust during Chinese New Year. To estimate the contribution of pyrotechnic events to Pb pollution in road dust, we used a simple binary model based on the ratios of $^{208}Pb/^{206}Pb$ (Cheng and Hu, 2010; Li et al., 2012; Liu et al., 2014). Aged dust Pb (background Pb) and pyrotechnic ash Pb (pyrotechnic Pb input) were set as the two end-member sources of Pb in pyrotechnic-influenced dust samples. Thus, the contribution of pyrotechnic events to road dust (X_{pyro}, %) could be expressed as Eq. (7).

$$X_{pyro}\% = \frac{(^{208}Pb/^{206}Pb)_{pyro-dust} - (^{208}Pb/^{206}Pb)_{aged-dust}}{(^{208}Pb/^{206}Pb)_{pyro} - (^{208}Pb/^{206}Pb)_{aged-dust}} \times 100 \quad (7)$$

where X_{pyro} represents the contribution of Pb from pyrotechnic events; while $(^{208}Pb/^{206}Pb)_{pyro\text{-}dust}$, $(^{208}Pb/^{206}Pb)_{aged\text{-}dust}$ and $(^{208}Pb/^{206}Pb)_{pyro}$ represent the Pb isotope ratio ($^{208}Pb/^{206}Pb$) in pyrotechnic-influenced dust, aged road dust and pyrotechnic ash samples, respectively. According to this binary model, pyrotechnic events contributed 41.3%, 34.3% and 55.7% of the Pb to road dust at sites LD, SJZ and CS, respectively. The contribution rates of pyrotechnic Pb to road dust in southern cities (LD and CS) were significantly higher than in the northern city (SJZ). This is consistent with estimates based on Sr concentrations, implying Pb emitted from pyrotechnic events is an important source of Pb in road dust of southern China.

3.3.3. Positive matrix factorization analysis

PMF analysis was carried out in conjunction with other qualitative analyses in this study to quantitively calculate pyrotechnic source contributions for each PTM. Following pyrotechnic displays, our PMF analysis identified four main factors affecting the accumulation of PTMs

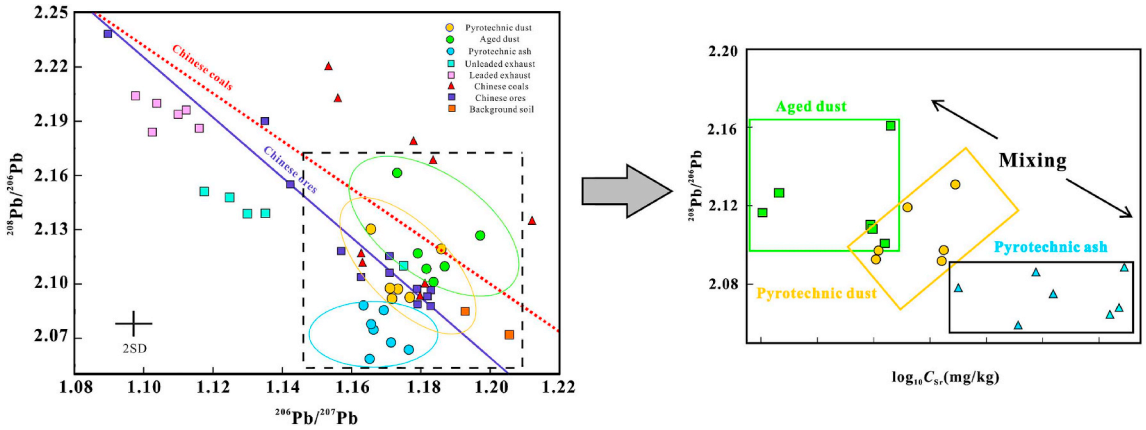

Fig. 3. Diagram of $^{208}Pb/^{206}Pb$ ratios against $^{206}Pb/^{207}Pb$ ratios found in pyrotechnic ashes, pyrotechnic-influenced dust and aged dust and scatter plot of $^{208}Pb/^{206}Pb$ ratios vs $\log_{10}C_{Sr}$ in aged dust, pyrotechnic-influenced dust and pyrotechnic ashes from our eight sampling sites throughout China. Data for other related sources are shown from Bi et al. (2017).

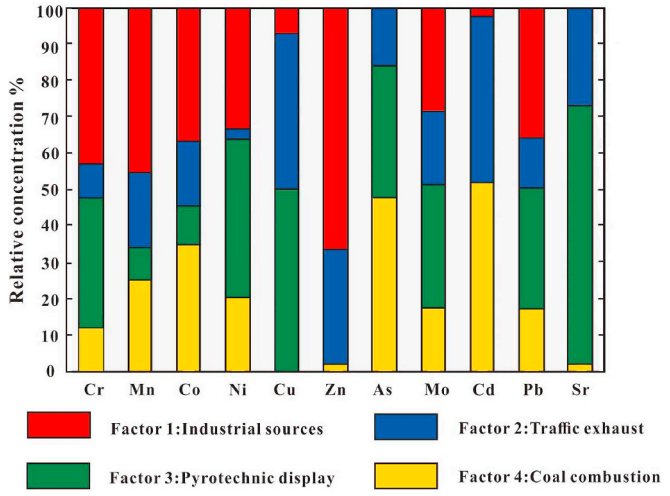

Fig. 4. Contributions of various sources to the measured potentially toxic metals in road dust after pyrotechnic displays.

in road dust (Fig. 4, Fig. S3). Factor 1 contributed 69.5%, 41.5%, 43.1% and 35.0% of the Zn, Cr, Mn and Pb to road dust samples, respectively. Typically, both steel and iron-ore processing emit Pb, Zn, Mn and other PTM pollutants (Duan and Tan, 2013; Fang et al., 2016). In addition, smelting and steel-processing plants are the main sources of atmospheric Cr (Duan and Tan, 2013). All these PTM pollutants could be accumulated in road dust through atmospheric deposition (Lv et al., 2006). In northwestern China, steel-processing plants are the main sources of Cr and Zn, yielding a high correlation between these elements ($r^2 = 0.74$, $p < 0.01$) (Chen et al., 2016b). Therefore, metal-smelting and processing are likely represented by this factor, given its association of elements.

Factor 2 accounted for 48.0%, 44.3% and 33.1% of the Cd, Cu and Zn in road dust samples. Cd is an important element in tires and lubricating oils, while Zn and Cu are key tracers of non-exhaust traffic sources (Duan and Tan, 2013; Pant and Harrison, 2013). Around 23.7% of Mn and 28.1% of Sr were likely associated with a gasoline source (Lin et al., 2005). Thus, this factor may represent traffic-related sources.

Factor 3 contributed 70.1% and 50.4% of the Sr and Cu to road dust samples. In addition, this factor was associated with moderate percentages of Pb (35.5%), Mo (36.6%), Ni (46.3%) and Cr (42.9%). Previously, high concentrations of Sr, Pb and Cu were associated with fireworks (Cao et al., 2017; Moreno et al., 2010). Moreover, according to qualitative analyses in this study, Cu, Cr and Sr were identified as being components of pyrotechnic devices and elevated in road dust after pyrotechnic displays. Thus, this factor could represent pyrotechnic emissions during Chinese New Year. Moreover, a small number of fireworks (e.g., JHQJ and HDY) contained plenty of Mo and Ni (Table 1), which would explain why factor 3 influences the concentrations of Mo and Ni in road dust after pyrotechnic events.

Factor 4 contributed 48.0%, 45.1%, 37.4% and 26.7% of the Cd, As, Co and Mn to road dust. Other studies found that these elements were linked to coal combustion (Deng et al., 2014; Men et al., 2018; Raja et al., 2014; Yang et al., 2014a; Zhao et al., 2017). Coal combustion emits fly ash into the atmosphere, whereby As and other related metals contained in the fly ash are deposited as road dust (Raja et al., 2014). Deng et al. (2014) found that fly ash from coal combustion sources had high values of Cd and Mn (Deng et al., 2014). Co compounds also are widely used as catalysts to remove Hg and other pollutants in coal flue gases, making this element a by-product of coal combustion activities (Yang et al., 2014a). It is worth noting that Cr and Pb are trace elements of coal combustion (Deng et al., 2014; Zhao et al., 2017). However, in this study, only 10.8% of the Cr and 17.6% of the Pb in pyrotechnic-influenced dust were likely derived from coal combustion. This suggests that pyrotechnic events emitted large amounts of Cr and Pb, diluting their contributions from coal combustion. Therefore, this factor could well represent coal combustion sources.

From the above discussion, we surmise that in the road dust samples collected after pyrotechnics display, pyrotechnic sources contributed about 70.1% of the Sr, 50.4% of the Cu, 46.3% of the Ni, 42.9% of the Cr, 36.6% of the Mo, 35.5% of the Pb, and 34.7% of the As, but contributed little to Mn, Co, Zn and Cd values (Fig. 4). This agrees well with PTM values in pyrotechnic ash. Our results suggest that PTMs, like Cr, Cu and Pb, emitted during pyrotechnic events may have been overlooked in previous assessments of road dust PTM pollution sources.

3.4. Human risk assessment and source-specific contributions

In road dust, Cr, Ni, Cu, Zn and Pb were the most concerning PTMs (Hu et al., 2015). Thus, these five PTMs were used to investigate the effect of the contribution of pollution from pyrotechnic displays to road dust and its related risks. To evaluate the contribution of pyrotechnic events to PTM-related risks of road dust, the oral-bioaccessibility values of PTMs in road dust, before and after pyrotechnic events, were measured to provide a source-specific risk assessment. Bioaccessibility (%) values of these PTMs in road dust, before and after pyrotechnic events, were ranked as Zn > Pb > Cu > Ni > Cr in both cases (Table S8). As shown in Table 2, health risks related to exposure to road dust for each PTM increased after pyrotechnic events. Moreover, the contributions of ingestion, inhalation and dermal contact to health risks (i.e., to the hazard quotient; HQ) of all PTMs (except Cr) reflected the order: $HQ_{ing} > HQ_{inh} > HQ_{derm}$ (Table S9, Table S10), consistent with previous studies (Li et al., 2017a; Xiao et al., 2017). This suggests that ingestion is the main exposure pathway to PTMs in road dust. The risk levels of non-carcinogenic PTMs were: Pb > Cr > Cd > Zn > Cu > Ni; while those of carcinogenic PTMs were: Ni > Cr > Cd (Table 2). Although non-carcinogenic risks values for all PTMs were lower than 1 and carcinogenic risk values were lower than 1E-06, we noted that both non-carcinogenic and carcinogenic risks were elevated after pyrotechnic events.

Using source profiles identified by the PMF after pyrotechnic events, we translated element-specific risks into source-specific risks (Table S11). In this way, the contribution of each source to human health risks

Table 2
Non-carcinogenic and carcinogenic risks for human exposure to road dust.

HI and Risks		Cr[a]	Ni[a]	Cd[a]	Cu	Zn	Pb	Total risks
Non-Carcinogenic risks								
Children	HI before fireworks	4.26E-02	1.60E-03	8.01E-03	4.53E-03	6.16E-03	8.90E-02	1.52E-01
	HI after fireworks	6.60E-02	2.04E-03	1.51E-02	3.69E-03	5.34E-03	9.32E-02	1.85E-01
Adult	HI before fireworks	6.07E-03	1.77E-04	8.74E-04	4.93E-04	6.68E-04	9.88E-03	1.81E-02
	HI after fireworks	9.54E-03	2.25E-04	1.43E-03	4.07E-04	5.79E-04	1.01E-02	2.23E-02
Carcinogenic risks								
	Risk before fireworks	9.32E-08	2.80E-07	2.69E-10				3.73E-07
	Risk after fireworks	1.51E-07	3.71E-07	3.85E-10				5.26E-07

[a] represents a carcinogenic metal HI represents Hazard Index.

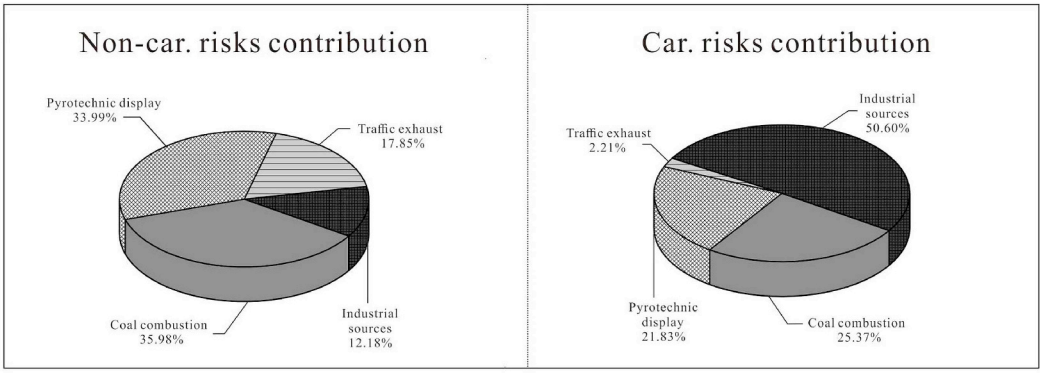

Fig. 5. Contribution of each source to non-carcinogenic risks and carcinogenic risks related to potentially toxic metals in road dusts following pyrotechnic events.

was calculated according to the PMF source apportionment (SI: Details of health risk assessment). As shown in Fig. 5, contributions from coal combustion (35.98%) and pyrotechnic displays (33.99%) were the dominant sources involved in determining non-carcinogenic risks. In contrast, the contributions of diverse sources to carcinogenic risks showed that industrial-related sources (50.6%), pyrotechnic events (21.83%) and coal combustion (25.37%) were most important. Previous studies reported that coal combustion, traffic exhaust and industrial sources were the main contributors to PTM exposure (Huang et al., 2018; Lin et al., 2017; Wang et al., 2016). In contrast, our study identified pyrotechnic sources as an important contributor to health risks, related to exposure to PTMs in road dust following pyrotechnic events, especially during Chinese New Year.

4. Conclusions

Pyrotechnic events may provide one of the major pathways of PTM exposure during celebrations worldwide, especially in China. Therefore, such events have become an emerging concern, because they emit PTMs not only as aerosols but also as particles that may be deposited as road dust. Our results indicated that the levels of Cu, Cr, Pb and Sr in pyrotechnic ash were high, causing all these PTMs in road dust to be elevated after pyrotechnic events. Our combined use of Pb isotopes and Sr values to trace pyrotechnic source material in road dust demonstrated that the Pb isotope signatures of pyrotechnic devices were distinguishable from other anthropogenic sources. Meanwhile, our PMF model confirmed that there was a recognizable effect of pyrotechnic sources on PTM values in road dust following pyrotechnic events. Using these data, our source-specific risk assessment indicated that pyrotechnic events contributed 33.99% (7.04E-02) to the non-carcinogenic risks and 21.83% (1.14E-07) to the carcinogenic risks related to exposure to PTMs in road dust. These findings help quantify the unusual sources of PTMs in road dust and the impact of pyrotechnic activities on human health.

Acknowledgements

This study was supported by the National Natural Science Foundation of China (No. 41773112) and Fundamental Research Funds for the Central Universities awarded to the China University of Geosciences (Wuhan) (CUGL160403, CUGCJ1703).

Appendix A. Supplementary data

Supplementary data to this article can be found online at https://doi.org/10.1016/j.ecoenv.2019.109604.

References

Azhagurajan, A., Selvakumar, N., Suresh, A., 2014. Environment friendly fireworks manufacturing using nano scale flash powder. J. Sci. Ind. Res. 73, 479–484.
Baranyai, E., Simon, E., Braun, M., Posta, J., Fábián, I., 2015. The effect of a fireworks event on the amount and elemental concentration of deposited dust collected in the city of Debrecen, Hungary. Air Qual. Atmos. Health 8, 359–365.
Bi, X., Li, Z., Sun, G., Liu, J., Han, Z., 2015. In vitro bioaccessibility of lead in surface dust and implications for human exposure: a comparative study between industrial area and urban district. J. Hazard Mater. 297, 191–197.
Bi, X., Li, Z., Wang, S., Zhang, L., Xu, R., Liu, J., Yang, H., Guo, M., 2017. Lead isotopic compositions of selected coals, Pb/Zn ores and fuels in China and the application for source tracing. Environ. Sci. Technol. 51, 13502–13508.
Cao, X., Zhang, X., Daniel, Q.T., Chen, W., Zhang, S., Zhao, H., Xiu, A., 2017. Review on physicochemical properties of pollutants released from fireworks: environmental and health effects and prevention. Environ. Rev. 26, 133–155.
Chen, T., Chang, Q., Liu, J., Clevers, J.G.P.W., Kooistra, L., 2016b. Identification of soil heavy metal sources and improvement in spatial mapping based on soil spectral information: a case study in northwest China. Sci. Total Environ. 565, 155–164.
Chen, Y., Schleicher, N., Fricker, M., Cen, K., Liu, X.L., Kaminski, U., Yu, Y., Wu, X.F., Norra, S., 2016a. Long-term variation of black carbon and PM2.5 in Beijing, China with respect to meteorological conditions and governmental measures. Environ. Pollut. 212, 269–278.
Cheng, H., Hu, Y., 2010. Lead (Pb) isotopic fingerprinting and its applications in lead pollution studies in China: a review. Environ. Pollut. 158, 1134–1146.
CNEMC (China National Environmental Monitoring Center), 1990. Background Concentrations of Elements of Soils in China. Chinese Environment Science Press, Beijing (in Chinese).
Comero, S., Vaccaro, S., Locoro, G., De, C.L., Gawlik, B.M., 2014. Characterization of the Danube river sediments using the PMF multivariate approach. Chemosphere 95, 329–335.
Crespo, J., Yubero, E., Nicolás, J.F., Lucarelli, F., Nava, S., Chiari, M., Calzolai, G., 2012. High-time resolution and size-segregated elemental composition in high-intensity pyrotechnic exposures. J. Hazard Mater. 241–242, 82–91.
Cundy, A.B., Croudace, I.W., 2017. The fate of contaminants and stable Pb isotopes in a changing estuarine environment: 20 years on. Environ. Sci. Technol. 51 (17), 9488–9497.
Das, A., Patel, S.S., Kumar, R., Krishna, K.V.S.S., Dutta, S., Saha, M.C., Sengupta, S., Guha, D., 2018. Geochemical sources of metal contamination in a coal mining area in Chhattisgarh, India using lead isotopic ratios. Chemosphere 197, 152–164.
Deng, S., Shi, Y., Liu, Y., Zhang, C., Zhang, F., 2014. Emission characteristics of Cd, Pb and Mn from coal combustion: field study at coal-fired power plants in China. Fuel Process. Technol. 126, 469–475.
Duan, J., Tan, J., 2013. Atmospheric heavy metals and Arsenic in China: situation, sources and control policies. Atmos. Environ. 74, 93–101.
Ettler, V., Cihlová, M., Jarošíková, A., Mihaljevič, M., Drahota, P., Kříbek, B., Vaněk, A., Penížek, V., Sracek, O., Klementová, M., Engel, Z., Kamona, F., Mapani, B., 2019. Oral bioaccessibility of metal(loid)s in dust materials from mining areas of northern Namibia. Environ. Int. 124, 205–215.
Fang, G.C., Zhuang, Y.J., Kuo, Y.C., Cho, M.H., 2016. Ambient air metallic elements (Mn, Fe, Zn, Cr, Cu, and Pb) pollutants sources study at a rural resident area near Taichung thermal power plant and industrial park: 6-month observations. Environ. Earth Sci. 75, 587–598.
Gao, P., Guo, H., Zhang, Z., Ou, C., Hang, J., Fan, Q., He, C., Wu, B., Feng, Y., Xing, B., 2018. Bioaccessibility and exposure assessment of trace metals from urban airborne particulate matter (PM10 and PM2.5) in simulated digestive fluid. Environ. Pollut. 242, 1669–1677.
Gunawardana, C., Goonetilleke, A., Egodawatta, P., Dawes, L., Kokot, S., 2012. Source characterization of road dust based on chemical and mineralogical composition. Chemosphere 87, 163–170.
Gurugubelli, B., 2014. Depawali Festival Day lead concentration in air-a case study. J. Agric. Life Sci. 1, 71–76.
Hu, B., Liu, B., Zhou, J., Guo, J., Sun, Z., Meng, W., Guo, X., Duan, J., 2015. Health risk assessment on heavy metals in urban street dust of Tianjin based on trapezoidal fuzzy

numbers. Hum. Ecol. Risk Assess. 22, 678–692.
Huang, R.J., Cheng, R., Jing, M., Yang, L., Li, Y., Chen, Q., Chen, Y., Lin, C., Wu, Y., Zhang, R., EI, H., Prevot, A., O'Dowd, C., Cao, J., 2018. Source-specific health risk analysis on particulate trace elements: coal combustion and traffic emission as major contributors in Winter time Beijing. Environ. Sci. Technol. 52, 10967–10974.
Jing, H., Li, Y.F., Zhao, J., Li, B., Sun, J., Chen, R., Gao, Y., Chen, C., 2014. Wide-range particle characterization and elemental concentration in Beijing aerosol during the 2013 Spring Festival. Environ. Pollut. 192, 204–211.
Keshavarzi, B., Tazarvi, Z., Rajabzadeh, M., Najmeddin, A., 2015. Chemical speciation, human health risk assessment and pollution level of selected heavy metals in urban street dust of Shiraz, Iran. Atmos. Environ. 119, 1–10.
Li, F.L., Liu, C.Q., Yang, Y.G., Bi, X.Y., Liu, T.Z., Zhao, Z.Q., 2012. Natural and anthropogenic lead in soils and vegetables around Guiyang city, southwest China: a Pb isotopic approach. Sci. Total Environ. 431, 339–347.
Li, H., Chen, L., Yu, L., Guo, Z., Shan, C., Lin, J., Gu, Y., Yang, Z., Yang, Y., Shao, J., Zhu, X., Cheng, Z., 2017a. Pollution characteristics and risk assessment of human exposure to oral bioaccessibility of heavy metals via urban street dusts from different functional areas in Chengdu, China. Sci. Total Environ. 586, 1076–1084.
Li, J., Xu, T., Lu, X., Chen, H., Nizkorodov, S., Chen, J., Yang, X., Mo, Z., Chen, Z., Liu, H., Mao, J., Liang, G., 2017b. Online single particle measurement of fireworks pollution during Chinese New Year in Nanning. J. Environ. Sci. 3, 184–195.
Li, T., Sun, G., Yang, C., Liang, K., Ma, S., Huang, L., Luo, W., 2019. Source apportionment and source-to-sink transport of major and trace elements in coastal sediments: combining positive matrix factorization and sediment trend analysis. Sci. Total Environ. 651, 344–356.
Lin, C.C., Chen, S.J., Huang, K.L., Hwang, W.I., Chang-Chien, G.P., Lin, W.Y., 2005. Characteristics of metals in nano/ultrafine/fine/coarse particles collected beside a heavily trafficked road. Environ. Sci. Technol. 39, 8113–8122.
Lin, M., Gui, H., Wang, Y., Peng, W., 2017. Pollution characteristics, source apportionment, and health risk of heavy metals in street dust of Suzhou, China. Environ. Sci. Pollut. Res. Int. 24, 1987–1998.
Liu, E., Yan, T., Birch, G., Zhu, Y., 2014. Pollution and health risk of potentially toxic metals in urban road dust in Nanjing, a mega-city of China. Sci. Total Environ. 476–477, 522–531.
Luo, X.S., Xue, Y., Wang, Y.L., Cang, L., Xu, B., Ding, J., 2015. Source identification and apportionment of heavy metals in urban soil profiles. Chemosphere 127, 152–157.
Luo, X.S., Yu, S., Li, X.D., 2011. Distribution, availability, and sources of trace metals in different particle size fractions of urban soils in Hong Kong: implications for assessing the risk to human health. Environ. Pollut. 159, 1317–1326.
Luo, X., Yu, S., Zhu, Y., Li, X., 2012. Trace metal contamination in urban soils of China. Sci. Total Environ. 421–422, 17–30.
Luo, X., Zhao, Z., Xie, J., Luo, J., Chen, Y., Li, H., Jin, L., 2019. Pulmonary bioaccessibility of trace metals in PM2.5 from different megacities simulated by lung fluid extraction and DGT method. Chemosphere 218, 915–921.
Lv, W., Wang, Y.X., Querol, X., Zhuang, X.G., Alastuey, A., Lopez, A., Viana, M., 2006. Geochemical and statistical analysis of trace metals in atmospheric particulates in Wuhan, central China. Environ. Geol. 51, 121–132.
Martinez-Haro, M., Taggart, M.A., Rosa, R.C., Martín-Doimeadiøs, Green, A.J., Mateo, R., 2011. Identifying sources of Pb exposure in water birds and effects on porphyrin metabolism using noninvasive fecal sampling. Environ. Sci. Technol. 45, 6153–6159.
Men, C., Liu, R., Xu, F., Wang, Q., Guo, L., Shen, Z., 2018. Pollution characteristics, risk assessment, and source apportionment of heavy metals in road dust in Beijing, China. Sci. Total Environ. 612, 138–147.
Moreno, T., Querol, X., Alastuey, A., Amato, F., Pey, J., Pandolfi, M., Kuenzli, N., Bouso, L., Rivera, M., Gibbons, W., 2010. Effect of fireworks events on urban background trace metal aerosol concentrations: is the cocktail worth the show? J. Hazard Mater. 183, 945–949.
Oomen, A.G., Hack, A., Minekus, M., Zeijdner, E., Cornelis, C., Schoeters, G., Versteraete, W., Vandewiele, T., Wraqq, J., Rompelberg, C., Sips, A., Vanwijnen, J., 2002. Comparison of five in vitro digestion models to study the bioaccessibility of soil contaminants. Environ. Sci. Technol. 36, 3326–3334.
Paatero, P., Tapper, U., 1994. Positive matrix factorization: a non-negative factor model with optimal utilization of error estimates of data values. Environmetrics 5, 111–126.
Padoan, E., Rome, C., Ajmone-Marsan, F., 2017. Bioaccessibility and size distribution of metals in road dust and roadside soils along a peri-urban transect. Sci. Total Environ. 601, 89–98.
Pant, P., Harrison, R.M., 2013. Estimation of the contribution of road traffic emissions to particulate matter concentrations from field measurements: a review. Atmos. Environ. 77, 78–97.
Pongpiachan, S., Hattayanone, M., Suttinun, O., Khumsup, C., Kittikoon, I., Hirunyatrakul, P., Cao, J., 2017a. Assessing human exposure to pm10-bound polycyclic aromatic hydrocarbons during fireworks displays. Atmos. Pollut. Res. 8, 816–827.
Pongpiachan, S., Iijima, A., 2016. Assessment of selected metals in the ambient air PM10 in urban sites of Bangkok (Thailand). Environ. Sci. Pollut. Res. 23, 2948–2961.
Pongpiachan, S., Iijima, A., Cao, J., 2018. Hazard quotients, hazard indexes, and cancer risks of toxic metals in PM10 during firework displays. Atmosphere 9, 144.
Pongpiachan, S., Kositanont, C., Palakun, J., Liu, S., Ho, K.F., Cao, J., 2015. Effects of day-of-week trends and vehicle types on PM2.5-bounded carbonaceous compositions. Sci. Total Environ. 532, 484–494.
Pongpiachan, S., Liu, S., Huang, R., Zhao, Z., Palakun, J., Kositanont, C., Cao, J., 2017b. Variation in day-of-week and seasonal concentrations of atmospheric PM2.5-bound metals and associated health risks in Bangkok, Thailand. Arch. Environ. Contam. Toxicol. 72, 364–379.
Pongpiachan, S., Paowa, T., 2014. Hospital out-and-in-patients as functions of trace gaseous species and other meteorological parameters in chiang-mai, Thailand. Aerosol Air Qual. Res. 15, 479–493.
Raja, R., Nayak, A.K., Rao, K.S., Puree, C., Shahid, M., Panda, B.B., Kumar, A., Tripathi, R., Bhattacharyya, P., Baig, M.J., Lal, B., Moh, S., Gautam, P., 2014. Effect of fly ash deposition on photosynthesis, growth and yield of rice. Bull. Environ. Contam. Toxicol. 93, 106–112.
Tang, X.Y., Luo, L., Cao, J.J., Wang, Q.Y., 2013. Characteristics of chemical elements in atmospheric PM2.5 during the Chinese New year in Chengdu. Environ. Sci. Technol. 5, 151–170.
Tian, Y., Shi, G., Han, S., Zhang, Y., Feng, Y., Liu, G., Gao, L., Wu, J., Zhu, T., 2013. Vertical characteristics of levels and potential sources of water-soluble ions in PM10 in a Chinese megacity. Sci. Total Environ. 447, 1–9.
Tsai, H.H., Chen, L.H., Yuan, C.S., Lin, Y.C., Jen, Y.H., IE, I.R., 2012. Influences of fireworks on chemical characteristics of atmospheric fine and coarse particles during Taiwan's. Lantern Festival. Atmos. Environ. 62, 256–264.
USEPA, 1989. Risk Assessment Guidance for Superfund. Human Health Evaluation Manual, (Part A) Vol.1 EPA/540/1-89/002. Office of Emergency and Remedial Response.
Vecchi, R., Bernardoni, V., Cricchio, D., D'Alessandro, A., Fermo, P., Lucarelli, F., Nava, S., Piazzalunga, A., Valli, G., 2008. The impact of fireworks on airborne particles. Atmos. Environ. 42, 1121–1132.
Wang, J., Li, S., Cui, X., Li, H., Qian, X., Wang, C., Sun, Y., 2016. Bioaccessibility, sources and health risk assessment of trace metals in urban park dust in Nanjing, Southeast China. Ecotoxicol. Environ. Saf. 128, 161–170.
Widory, D., Liu, X., Dong, S., 2010. Isotopes as tracers of sources of lead and strontium in aerosols (TSP & PM2.5) in Beijing. Atmos. Environ. 44, 3679–3687.
Xiao, R., Wang, S., Li, R., Wang, J.J., Zhang, Z., 2017. Soil heavy metal contamination and health risks associated with artisanal gold mining in Tongguan, Shaanxi, China. Ecotoxicol. Environ. Saf. 141, 17–24.
Yang, J., Zhao, Y., Zhang, J., Zheng, C., 2014a. Regenerable cobalt oxide loaded magnetosphere catalyst from fly ash for mercury removal in coal combustion flue gas. Environ. Sci. Technol. 48, 14837–14843.
Yang, L., Gao, X., Wang, X., Wei, N., Wang, J., Gao, R., Xu, P., Shou, Y., Zhang, Q., Wang, W., 2014b. Impacts of firecracker burning on aerosol chemical characteristics and human health risk levels during the Chinese New Year Celebration in Jinan, China. Sci. Total Envirno. 476–477, 57–64.
Yu, W., Liu, R., Xu, F., Men, C., Shen, Z., 2016b. Identifications and seasonal variations of sources of polycyclic aromatic hydrocarbons (PAHs) in the Yangtze River Estuary, China. Mar. Pollut. Bull. 104, 347–354.
Yu, Y., Ma, J., Song, N., Wang, X., Wei, T., Yang, Z., Li, Y., 2016a. Comparison of metal pollution and health risks of urban dust in Beijing in 2007 and 2012. Environ. Monit. Assess. 188, 657–667.
Zhang, J., Yang, L., Chen, J., Mellouki, A., Jiang, P., Gao, Y., Li, Y., Yang, Y., Wang, W., 2016. Influence of fireworks displays on the chemical characteristics of PM2.5 in rural and suburban areas in Central and East China. Sci. Total Environ. 578, 476–484.
Zhao, Y., Yang, J., Ma, S., Zhang, S., Zheng, C., 2017. Emission controls of mercury and other trace elements during coal combustion in China: a review. Int. Geol. Rev. 60, 638–670.